

ORIGINAL ARTICLE

Phenotypic and transcriptomic analysis reveals key genes associated with plant height in rubber tree and functional characterization of the candidate gene *HbFLA11*

Baoyi Yang^{1,2,3} | Yuanyuan Zhang¹ | Weiguo Li¹ | Xiao Huang¹ | Xinsheng Gao¹ | Juncang Qi²  | Xiangjun Wang¹ 

¹Rubber Research Institute, Chinese Academy of Tropical Agricultural Sciences, Haikou, China

²Agricultural College of Shihezi University/The Key Laboratory of Oasis Eco-agriculture, Xinjiang Production and Construction Group, Shihezi, China

³Research Institute of Crops, Xinjiang Academy of Agricultural Sciences, Urumqi, China

Correspondence

Juncang Qi, Agricultural College of Shihezi University, North Fourth Road, Shihezi City, Xinjiang Uyghur Autonomous Region, China. Email: qjc_agr@shzu.edu.cn

Xiangjun Wang, Rubber Research Institute, Chinese Academy of Tropical Agricultural Sciences, No. 4, Xueyuan Road, Longhua District, Haikou City, Hainan Province, China. Email: hnwxj@catas.cn

Assigned to Associate Editor Awais Khan.

Funding information

Central Public-interest Scientific Institution Basal Research Fund, Grant/Award Number: No. 1630032022007; Special Fund for Hainan Excellent Team 'Rubber Genetics and Breeding', Grant/Award Number: 20210203

Abstract

The rubber tree (*Hevea brasiliensis*) is an important species in global natural rubber production. However, the mechanisms regulating the height of rubber trees remain poorly understood. In previous work, the dwarf mutant MU73397 was obtained through ethyl methanesulfonate mutagenesis. Compared to the wild-type CATAS73397, MU73397 exhibited significantly reduced plant height and stem diameter, slower xylem development, and decreased cellulose and lignin content. Phytohormone analysis revealed that gibberellin levels were reduced in both the apex and stem of MU73397, while jasmonic acid was increased in the apex and auxin was reduced in the stem. These differences in hormone levels may contribute to the dwarf phenotype. Transcriptome analysis identified nine key genes related to cell wall biosynthesis and hormone signaling, namely, *FLA11* (Fasciclin-like arabinogalactan protein 11), *TUBB1* (Tubulin Beta 1), *TUBB6* (Tubulin Beta 6), *CESA7* (cellulose synthase A 7), *TUBA4* (Tubulin Alpha 4), *LAC17* (Laccase 7), *CTL2* (Chitinase-like protein 2), *IRX9* (Irregular xylem 9), and *KOR* (korrigan). Overexpression of *HbFLA11* in transgenic poplar resulted in significant increases in plant height and stem diameter. Gibberellin signaling genes and cell wall biosynthesis genes were significantly upregulated in the transgenic lines. These results suggest that *HbFLA11* is involved in gibberellin signaling and cell wall biosynthesis, thereby regulating plant growth. This study provides valuable genetic resources and research foundations for targeted trait breeding in rubber tree.

Abbreviations: FLA11, Fasciclin-like arabinogalactan protein 11; GA, gibberellin; KOR, korrigan; LB, Luria Broth; MS, Murashige and Skoog; TUBB1, Tubulin Beta 1; WT, wild type.

This is an open access article under the terms of the [Creative Commons Attribution-NonCommercial-NoDerivs](https://creativecommons.org/licenses/by-nc-nd/4.0/) License, which permits use and distribution in any medium, provided the original work is properly cited, the use is non-commercial and no modifications or adaptations are made.

© 2025 The Author(s). *The Plant Genome* published by Wiley Periodicals LLC on behalf of Crop Science Society of America.

Plain Language Summary

The plant height is an important factor influencing growth of rubber tree. However, the molecular mechanisms controlling plant height remain poorly understood. This study investigates the molecular mechanisms underlying the reduced height of the dwarf mutant MU73397. Hormonal and transcriptomic analyses identified key factors involved in growth regulation. Overexpression of the *HbFLA11* gene in transgenic poplar resulted in significant increases in plant height and stem diameter, providing valuable insights for genetic improvement strategies to enhance rubber tree growth.

1 | INTRODUCTION

The rubber tree (*Hevea brasiliensis*), indigenous to the Amazon basin in South America and belonging to the Euphorbiaceae family, was domesticated in the 1870s and subsequently transplanted to regions in Southeast Asia, West Africa, and South China. The natural rubber produced by rubber trees serves as a vital commodity in various industries, supplying raw materials for industrial, medical, agriculture, automobiles, aircraft, railways, textile, and sports industries and engineering sectors, as well as contributing to the construction of buildings and roads (Balai et al., 2023). Typically, rubber tree seedlings take approximately 5–6 years to meet latex production requirements, and the breeding cycle can last up to 30 years (Priyadarshan, 2022). A mature rubber tree can usually reach a height of 30 m. This is a huge challenge to the rubber tree's ability to withstand wind damage. Traditional production methods cannot effectively control the height of rubber tree.

Plant height influences plant structure and lodging resistance (G. L. Wang et al., 2017). For trees, it also serves as a major indicator of growth performance. The height of a plant not only affects its photosynthetic efficiency and resource utilization but also directly influences its structural stability. Particularly in the face of wind damage, taller trees are more prone to lodging, which can impact their growth and yield. As an important economic crop, the regulation of rubber tree height is crucial for improving its wind resistance. Excessive plant height can lead to wind damage-induced lodging, thereby affecting the growth and latex production of rubber trees. Therefore, studying the genes regulating plant height and their molecular mechanisms can help breed new rubber tree varieties with optimal height and enhanced wind resistance. Previous studies have revealed many genes associated with plant height through ethyl methanesulfonate (EMS) mutagenesis. For example, in the EMS-induced dwarf mutant (*dw*) of soybean Zhongpin 661 (ZDD23893), the reduced plant height is primarily caused by a shortening of cell length, which is related to a deficiency of gibberellin (GA). Exoge-

nous GA treatment can partially rescue this phenotype (Li et al., 2018). In wheat, an EMS-induced dwarf mutant was created, and it was found that the reduced plant height is linked to the GA signaling pathway. Through gene mapping, a new allele, *Rht-A1h*, associated with plant height regulation, was identified. This mutant showed lower sensitivity to exogenous GA but could still partially restore its plant height (Xie et al., 2024). Currently, some studies have explored the plant height regulation network of rubber tree based on genomics and growth phenotypes. In recent years, researchers in Malaysia (Rahman et al., 2013), China (Cheng et al., 2023; Tang et al., 2016), Japan (Lau et al., 2016), and Thailand (Pootakham et al., 2017) have generated and published insights into the rubber tree genome. Mapping of quantitative trait loci of growth phenotypes (Conson et al., 2018; Rosa et al., 2018), the construction of ultra-high-density genetic maps (W. Wu et al., 2022), and the establishment of biological networks between the phenotype and molecules through genome-wide association studies (GWAS) (Francisco et al., 2021) have provided a robust foundation for the discovery of genes related to plant height in rubber tree. But overall, in-depth research on rubber tree height genes is still lacking.

Plant height is closely related to the development of the cell wall. The secondary cell wall provides mechanical support, promotes vertical growth, and ensures the plant's stability and rigidity. The secondary cell wall represents a distinctive structure in woody plant cells, primarily comprised of cellulose, hemicellulose, and lignin (D. Zhang et al., 2018). Cellulose microfibrils form the foundational load-bearing network, which crosslinks with lignin and hemicellulose to create a rigid and tough support structure crucial for plant growth (Taylor-Teeples et al., 2015). This framework provides the necessary support for upright vertical growth, nutrient, and water transportation, and enables penetration through various tissues and organs (D. Zhang et al., 2018). Fasciclin-like arabinogalactan protein (FLA), a component of cell wall glycoproteins, plays a crucial role in cellulose formation (Liu et al., 2020). Both actively participate in the biosynthesis of

plant cell wall components. GA is recognized as a pivotal hormone involved in regulating the initiation, elongation, and thickness of secondary wall fibers (Tian et al., 2022). Studies indicate that GA stimulates fiber development in cotton by upregulating the abundance of *FLA* expression (Wang et al., 2017).

In previous studies, we obtained the dwarf mutant MU73397 by EMS mutagenesis of immature anthers of the Brazilian rubber tree cultivar CATAS73397. The plant height and stem diameter measurements showed that MU73397 was shorter than CATAS73397 and had a thinner stem. In this study, we conducted phenotypic characterization and comparative transcriptomic analysis of the dwarf mutant MU73397 generated. The study aim of this approach was to identify key genes involved in regulating the dwarf phenotype of MU73397. These findings provide new insights into the mechanisms controlling plant height.

2 | MATERIALS AND METHODS

2.1 | Plant materials

The high-yield rubber tree variety, CATAS73397, derived from the hybridization of RRIM600 and PR107, stands as one of the most extensively cultivated varieties in China. In the previous work, the immature anthers of CATAS73397 were induced into a callus on a modified Murashige and Skoog (MS) medium. Subsequently, these calluses were cultured on an embryo culture medium to generate primary embryos. These primary embryos were then used as explants to induce callus and regenerate embryos again (Hua et al., 2010). These regenerated embryos, termed secondary embryos, were chemically mutated by submerging them in a 0.5% EMS-phosphate buffer for 4 h. After the treatment, the embryos were cultured and regenerated into plants (Chen et al., 2012). Eventually, from these plants, we identified a mutant strain exhibiting significantly reduced growth rates. This mutant was designated as MU73397. The latent buds of MU73397 and CATAS73397 were grafted onto the rootstock to obtain grafted seedlings for subsequent experiments.

2.2 | Phenotypic measurement

The plant height and stem diameter of MU73397 and CATAS73397 were assessed 1 year after planting. Three plants of each cultivar were measured. Tree height was determined using a ruler, measuring the vertical distance from the soil surface to the highest point of the plant. Stem diameter was measured using a vernier caliper at a height of 30 cm above the plant base. Plant height of transgenic and wild-type poplar was measured 2 months after growth under greenhouse conditions, following the same method as described for rubber

Core Ideas

- The MU73397 exhibits characteristics such as thinner cell walls, smaller cell size, and reduced cellulose and lignin content.
- Gibberellin and auxin levels are decreased in MU73397, while jasmonic acid and other hormones are upregulated.
- Weighted gene co-expression network analysis identified key modules related to cell wall biosynthesis and nine critical genes.
- Overexpression of *HbFLA11* in poplar significantly increased plant height and is associated with gibberellin signaling and cell wall biosynthesis.

tree, with height measured from the soil surface to the highest point of the plant.

2.3 | Xylem structure observation

Stem segments from the base to 10 cm above the base of 1-month-old poplars grown in a greenhouse were collected for paraffin section preparation. The samples were fixed in formalin-acetic-alcohol (FAA) solution (75% ethanol, acetic acid, and formaldehyde mixed at a ratio of 90:5:5) at 4°C for 36 h. After fixation, the samples were stored in 75% ethanol. The samples were then dehydrated in a series of increasing ethanol concentrations (75%, 80%, 85%, 90%, 95%, and 100% v/v) and infiltrated with a series of xylene-ethanol mixtures (25%, 50%, 75%, and 100% xylene, v/v). After dehydration, the samples were embedded in paraffin and sectioned into 8 μm thick slices using a microtome (LEICA RM2265, Leica). The sections were dewaxed in xylene, stained with Safranin and Fast Green FCF, and observed and imaged using a Leica DCF500 optical microscope.

Stem segments from the base to 20 cm above the base were collected from 1-year-old MU73397 and CATAS73397, and the development of the xylem was observed using scanning electron microscopy (SEM). The sample preparation followed the procedure outlined by X. J. Wang et al. (2018). First, the stem segments were washed with 0.1 M PBS (phosphate-buffered saline) to remove surface contaminants. The samples were then fixed in 2.5% glutaraldehyde solution for 12 h at 4°C. After fixation, the samples were dehydrated using a gradient series of ethanol (50%, 70%, 80%, 90%, 95%, and 100%, v/v). Following dehydration, the stem segments were immersed in tert-butyl alcohol for 30 min, repeating this step three times to further dehydrate and prevent shrinkage. The samples were then subjected to critical point drying using

a LEICA EM CPD 300 (Wetzlar). After drying, the samples were sectioned transversely and coated with gold using a sputter coater. Finally, the specimens were observed and photographed under a scanning electron microscope (SEM, ZEISS EIGMA, ZEISS).

2.4 | Analysis of lignin and cellulose contents

Samples were prepared according to the requirements of GB/T 2677.1 (1993) (National Standard of the People's Republic of China). The young stems were ground into powder, ensuring that the particle size could pass through a 40-mesh sieve. The powdered samples were then dried in a baking oven (DHG-9203A, Wind Edge) and reserved for subsequent steps. Then, adhering to the GB/T 2677.6 (1994) method, resin was extracted from 1 g of the sample using a benzene-ethanol mixture (with a ratio of benzene to 95% ethanol being 2:1) in a Soxhlet extractor for a duration of 6 h. The extracted resin was then dried for later use.

The lignin content was subsequently measured using the procedure specified in GB/T 2677.8 (1994). Initially, 1 g of the dry sample (m_0) was put into a 100-mL Erlenmeyer flask. Subsequently, 15 mL of 72% sulfuric acid was added. This mixture was then placed in a water bath maintained at 20°C for a duration of 2 h. Then, the total volume of the solution was increased to 560 mL by adding distilled water into a 1000-mL Erlenmeyer flask. This solution was boiled for 4 h on a 300°C hot plate. Following vacuum filtration, the residue was rinsed with distilled water until it attained a state of neutrality and subsequently dehydrated in an oven until a constant weight (m_1) was achieved. The lignin content (X_1) was determined by the formula: $X_1 = m_1/m_0 \times 100$.

The cellulose content was measured following the procedure outlined in GB/T 2677.10 (1995). A gram of the dried specimen (M_0) was placed into a 250-mL Erlenmeyer flask, together with 65 mL of distilled water, 0.5 mL of glacial acetic acid, and 0.6 g of sodium chlorite. The mixture was subsequently placed in a water bath set to 75°C for a duration of 1 h. After this period, an additional 0.5 mL of glacial acetic acid and 0.6 g of sodium chlorite were introduced into the mixture, followed by another hour of incubation at 75°C in the water bath. This entire procedure was repeated four times in total. The residue obtained was filtered through a G2 glass filter, rinsed with acetone thrice, dried, and weighed (M_1). The total cellulose (X_1) content was calculated according to the formula: $X_1 = M_1/M_0 \times 100$. The experiment was conducted in triplicate for accuracy.

2.5 | Determination of phytohormones

The concentrations of 88 phytohormones, including auxin, cytokinin, and GA, present in the stem apex and young

stems of both MU73397 and CATAS73397 were determined using the LC-MS/MS method. The method started by rapidly freezing fresh plant samples in liquid nitrogen. The materials were then finely ground for 1 min at 30 Hz. Following this, 50 mg of the ground sample was precisely weighed and placed into a 2 mL plastic microtube. This tube was quickly frozen in liquid nitrogen before being mixed with 1 mL of a methanol/water/formic acid solution (15:4:1, V/V/V). Finally, 10 μ L of an internal standard solution, at a concentration of 100 ng/mL, was added to the resultant extract.

The mixture underwent vortexing for 10 min and was then centrifuged at 12,000 revolutions per minute at a temperature of 4°C for 5 min. After centrifugation, the supernatant was carefully moved into a clean plastic microtube. The resulting supernatant was subsequently evaporated until dry and then reconstituted in 100 μ L of 80% methanol (V/V). The concocted mixture was then filtered using a 0.22 μ m membrane filter in preparation for LC-MS/MS analysis. The analysis of the sample extracts was conducted using a UPLC-ESI-MS/MS system. This system was capable of performing scans in both positive and negative ion modes, using a triple quadrupole (QQQ)-linear ion trap (LIT) mass spectrometer (QTRAP), specifically the QTRAP 6500 + LC-MS/MS System. It was furnished with an ESI Turbo Ion Spray interface and operated using Analyst 1.6.3 software from Sciex. This setup allowed for the acquisition of both LIT and triple QQQ scans.

Data acquisition was conducted utilizing Analyst 1.6.3 software (Sciex), and the quantification of all metabolites was carried out utilizing MultiQuant 3.0.3 software (Sciex).

2.6 | Transcriptome sequencing and analysis

RNA-Seq analysis was conducted on the xylem and bark tissues obtained from both MU73397 and CATAS73397. Three replicates of the biological samples were used. The total RNAs obtained from these samples underwent rigorous assessment for quality, purity, and integrity. mRNA was separated from the total RNA using oligo(dT)-coated magnetic beads, which helped in enriching for mRNA sequences. The initial cDNA strand was synthesized via reverse transcription, using the isolated mRNA fragments as templates. Following the initial steps, the synthesis of the second-strand cDNA was carried out in a mixture containing DNA polymerase I, dNTPs, RNaseH, and buffer. After this process, RNA-seq libraries were formulated utilizing the NEBNext Ultra RNA Library Prep Kit specifically for Illumina sequencing and were subsequently sequenced on the Illumina HiSeq4000 platform. High-grade, pristine reads were obtained through the elimination of low-quality reads and the trimming of adapter sequences from the initial raw reads. The purified reads were matched against the reference genome (v 1) using

HISAT2 software (v 2.1.0, Johns Hopkins University). Raw sequencing data were deposited in the NCBI database under the accession number PRJNA1112341.

Gene expression quantification was performed by calculating the number of FPKMs, which represents the expected number of fragments per kilobase of transcript per million mapped fragments (Mortazavi et al., 2008). The DEGs between CATAS73397 and MU73397 were analyzed using the R package—DESeq2. A DEG was considered significantly and differentially expressed if $|\log_2(\text{FoldChange})| > 1$ and q value < 0.05 . According to Gene Ontology (GO) and Kyoto Encyclopedia of Genes and Genomes (KEGG) databases, the differential expression genes (DEGs) were annotated and clustered using the clusterProfiler software (v 4.1.1, Southern Medical University).

2.7 | Weighted gene co-expression network analysis (WGCNA)

The expression data (FPKM value) of all genes and the phenotype measurements (plant height and girth) were used for co-expression analysis. The construction of the co-expression network was accomplished utilizing the R package—WGCNA (v 1.6.9), from which hub genes were identified. The R software (v 4.2) was utilized to calculate the correlation coefficients among the hub genes within the module. Subsequently, the interaction network was visualized utilizing Cytoscape (v 3.8.2).

2.8 | Quantitative real-time PCR

Leaf samples from 1-year-old rubber tree and 1-month-old poplars grown in a greenhouse were collected for qRT-PCR analysis. Total RNA was extracted using the Plant RNA Rapid Extract Kit (Coolaber) and subsequently reverse transcribed into cDNA using the TransScript One-Step gDNA Removal and cDNA Synthesis SuperMix (TransGen). The qRT-PCR analysis was conducted with a PerfectStart Green qPCR SuperMix (TransGen) on a CFX96 Touch Real-Time PCR Detection System (CFX96, Bio-Rad). The primer sequences for all experiments were developed using Primer Premier software (v 5.0) and are detailed in Table S1. The *HbActin* and *PtActin* served as an internal control to normalize the expression levels of the gene of interest. All experimental samples were performed with six replicas, comprising three biological and three technical. Data results were examined through the $2^{-\Delta\Delta C_t}$ method.

2.9 | Transgenic experiment of poplar

To investigate the potential function of *HbFLA11* overexpression in transgenic poplar seedlings, the coding sequence

of *HbFLA11* (scaffold2580_7757) was obtained from the HeveaDB database (<http://hevea.catas.cn/home/index>). First, leaves from CATAS73397 were collected, total RNA was extracted, and cDNA was synthesized by reverse transcription. Specific primers were designed to amplify the full-length cDNA of the *HbFLA11* gene. The amplified product was then cloned into the pEarleyGate 100 vector using Exnase II (Vazyme). 1 μL of recombinant plasmid DNA was added to 50 μL of competent *Agrobacterium* cells GV3101, gently mixed, and subjected to electroporation. After adding 1 mL of Luria Broth (LB) medium, the mixture was incubated at 30°C with shaking at 180 rpm for 30 min to activate the bacteria. A 50 μL aliquot of the activated culture was plated on LB agar and incubated in the dark at 30°C for 48 h. Positive transformants were then expanded for subsequent genetic transformation of poplar.

The genetic transformation of poplar was conducted by Shanghai Waker Bioscience Co., Ltd. For the experiment, poplar plants aged 1–3 months with uniform leaf color were selected. The central part of the leaves was scarified and immersed in an *Agrobacterium* infection solution with an OD600 of 0.3–0.4. After shaking continuously for 15 min, the leaves were removed and placed in co-cultivation medium for 2 days under dark conditions at 25°C. The leaves were then transferred to wound-inducing medium for further incubation in the dark until callus formation, which could last up to 45 days. After callus differentiation, the tissues were transferred to rooting selection medium, and root development was observed after 7–15 days. Positive transgenic shoots were selected on MS agar plates containing 50 $\mu\text{g}/\text{mL}$ kanamycin, and PCR amplification of the target gene fragment was performed to verify the success of genetic transformation. The OE1, OE3, and OE4 lines were selected for further analysis.

2.10 | Statistical analysis

Statistical analyses were performed using SPSS version 17.0. Data were obtained from at least three biological replicates and are presented as mean values \pm standard deviations. Student's t -test was conducted to determine significant differences ($*p < 0.05$; $**p < 0.01$; $***p < 0.001$).

3 | RESULT

3.1 | Phenotypic characterization of dwarf mutant MU73397

Using EMS mutagenesis on immature anthers of the cultivated rubber tree variety CATAS73397, the dwarf mutant MU73397 was obtained (Chen et al., 2012). After 1 year of growth in the greenhouse, MU73397 exhibited slower growth and delayed development compared to CATAS73397

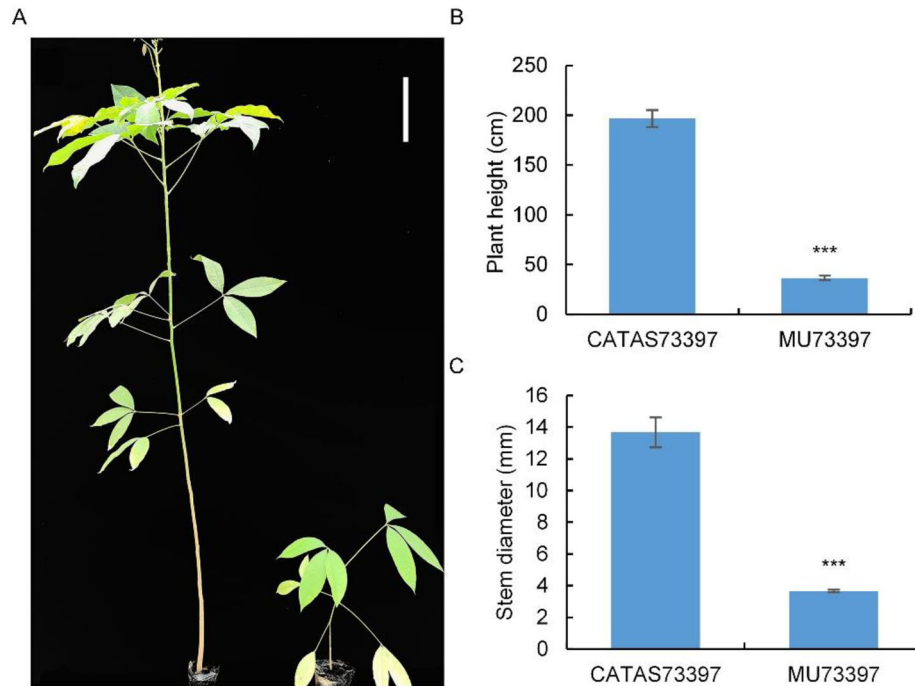


FIGURE 1 Differences in plant height and stem diameter between MU73397 and CATAS73397. (A) Images of MU73397 and CATAS73397 at 1 year of age. Bar = 20 cm. (B) Plant height of MU73397 and CATAS73397. (C) Stem diameter of MU73397 and CATAS73397. *** $p < 0.001$.

(Figure 1A). The plant height was measured as the vertical distance from the ground to the highest point of the plant. The results showed that the plant height of MU73397 was significantly reduced by 81.33% compared to the wild type (WT) plants (Figure 1B). At the same time, the stem diameter was measured 20 cm above the base of the plant, and the results indicated that the stem diameter of MU73397 was reduced by 73.15% (Figure 1C). These findings indicate that MU73397 experiences significant growth inhibition.

3.2 | Xylem developmental defects in the stem of MU73397

To further investigate the cause of dwarfism in MU73397, we excised the stems 20 cm above the base of the plant from both the MU73397 and CATAS73397, and observed the development of the xylem using SEM. The results revealed that xylem development in MU73397 was slower than in the control CATAS73397 (Figure 2A), with xylem width reduced by 50.38% in MU73397 compared to CATAS73397 (Figure 2B). These findings suggest that impaired xylem development is a key factor contributing to the dwarf phenotype of MU73397. Quantitative analysis of the major components of the xylem cell wall, cellulose and lignin, showed that the cellulose content in the xylem cell wall of MU73397 was 50.12%, compared to 65.22% in CATAS73397, a 15.1% reduction (Figure 2C). The lignin content was 21.76% in MU73397 and 29.06% in CATAS73397, representing a 7.3% decrease (Figure 2D). These results indicate a reduction in both cel-

lulose and lignin content in MU73397. The thickness of the xylem cell wall was measured. The thickness of the cell wall in MU73397 was approximately 1.17 μm , compared to 0.71 μm in CATAS73397, reflecting a 39.32% reduction (Figure 2E). This suggests that secondary wall thickening is delayed in MU73397. The number of xylem cell layers in cross sections was also reduced, with approximately 25 layers in MU73397 compared to 37 layers in CATAS73397, a decrease of about 12 layers (Figure 2F). These findings indicate impaired xylem cell differentiation and proliferation in MU73397. The size of the fiber cells, which play a crucial role in cell wall thickening, was measured. The average fiber cell length in MU73397 was 15.79 μm , compared to 20.57 μm in CATAS73397, a reduction of 23.23% (Figure 2G). Similarly, the average fiber cell width was 6.27 μm in MU73397, compared to 10.16 μm in CATAS73397, a reduction of 38.31% (Figure 2H). These results indicate a decrease in both the number and size of xylem cells in MU73397.

In conclusion, the dwarf phenotype of MU73397 is closely associated with delayed xylem development, reduced cell wall component levels, and altered cell wall structure. These changes collectively contribute to the significant reduction in plant height, stem diameter, and overall growth in MU73397.

3.3 | Differences in phytohormone levels between MU73397 and CATAS73397

To investigate the role of plant hormones in regulating the stem growth of MU73397, we quantified the levels of

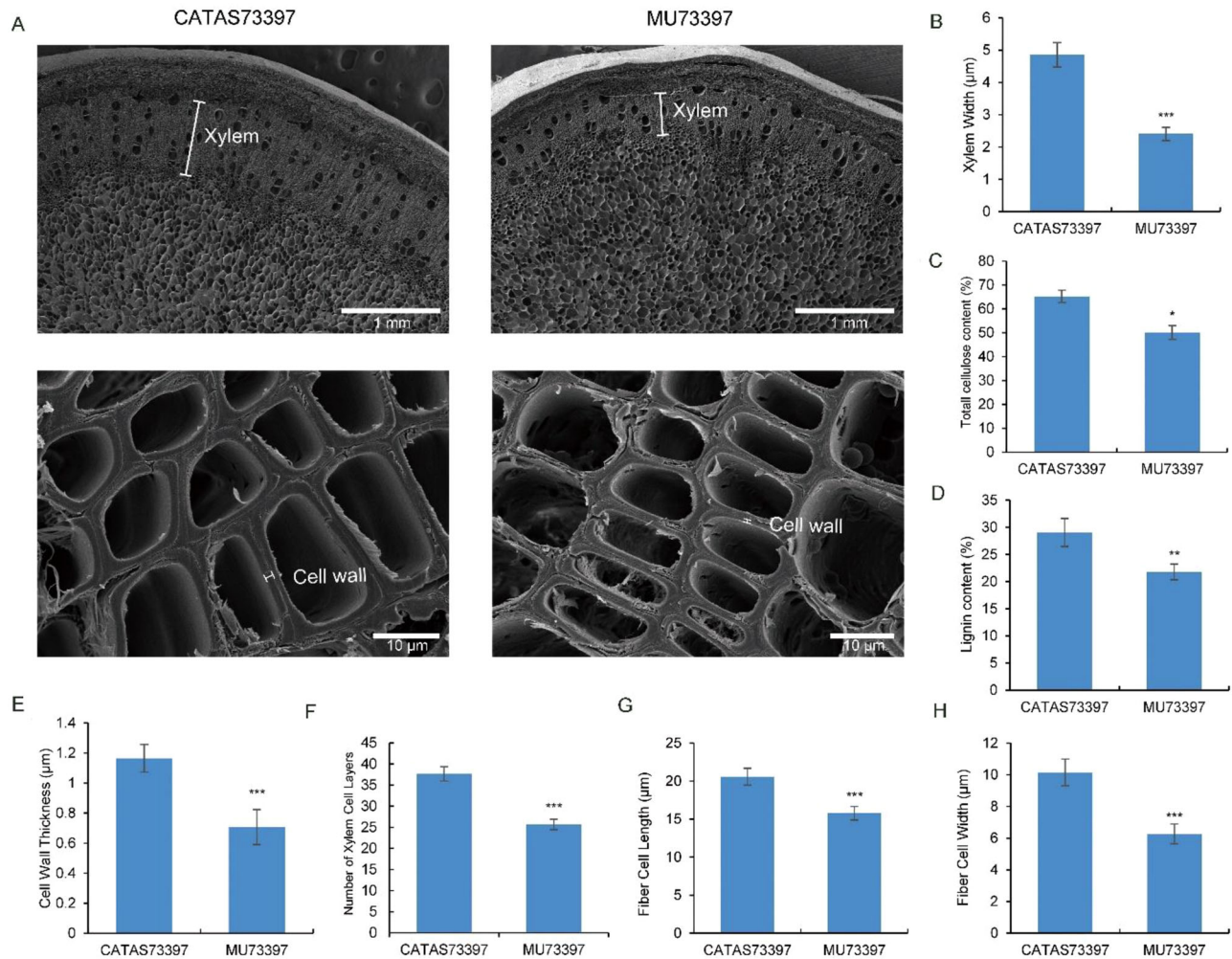


FIGURE 2 Differences in xylem development between MU73397 and CATAS73397. (A) Microscopic images of stem cross-sections taken 20 cm above the base of MU73397 and CATAS73397 of 1-year-old. White line segments indicate xylem width and cell wall thickness. Bar = 1 mm (upper images); bar = 10 μm (lower images). (B) Xylem width in MU73397 and CATAS73397. (C) Cellulose content in the xylem of MU73397 and CATAS73397. (D) Lignin content in the xylem of MU73397 and CATAS73397. (E) Cell wall thickness of fiber cells in the xylem of MU73397 and CATAS73397. (F) Number of cell layers of fiber cells in the xylem of MU73397 and CATAS73397. (G) Length of fiber cells in the xylem of MU73397 and CATAS73397. (H) Width of fiber cells in the xylem of MU73397 and CATAS73397. * $p < 0.05$; ** $p < 0.01$; *** $p < 0.001$.

plant hormones in the apex and the young stems 20 cm above the base of MU73397 and CATAS73397 (Figure 3). In the apex, the accumulation of 10 hormones showed significant differences (Figure 3A). Growth-promoting hormones exhibited an overall decreasing trend. Specifically, the contents of trans-Zeatin riboside (tZR), A3 (GA3), and A4 (GA4) in MU73397 apex were significantly lower than those in CATAS73397. Meanwhile, growth-inhibiting jasmonate hormones—jasmonoyl-L-isoleucine (JA-ILE), N-[(-)-jasmonoyl]-L-valine (JA-Val), jasmonic acid (JA), and 3-oxo-2-(2-(Z)-pentenyl) cyclopentane-1-butyric acid (OPC-4)—showed significant accumulation in MU73397 apex.

The hormonal differences were more pronounced in stem tissues, with a total of 18 differentially accumulated hormones detected (Figure 3B). A3 (GA3), GA A4, key components in auxin metabolic pathways (methyl indole-3-acetate, indole-3-

acetyl-L-aspartic acid, indole-3-carboxaldehyde, and indole-3-lactic acid), and the cytokinin N6-isopentenyladenine were significantly reduced in MU73397 stems. In conclusion, the differential accumulation levels of these hormones collectively contribute to the formation of the dwarf phenotype in MU73397.

3.4 | Comparative transcriptome analysis

To explore the molecular mechanisms underlying the dwarf phenotype of the MU73397 mutant, we collected xylem and bark from the stems 20 cm above the base of MU73397 and CATAS73397 and constructed cDNA libraries. Sequencing results showed that the average raw reads across all samples were 42,030,194, and after filtering, the average number of

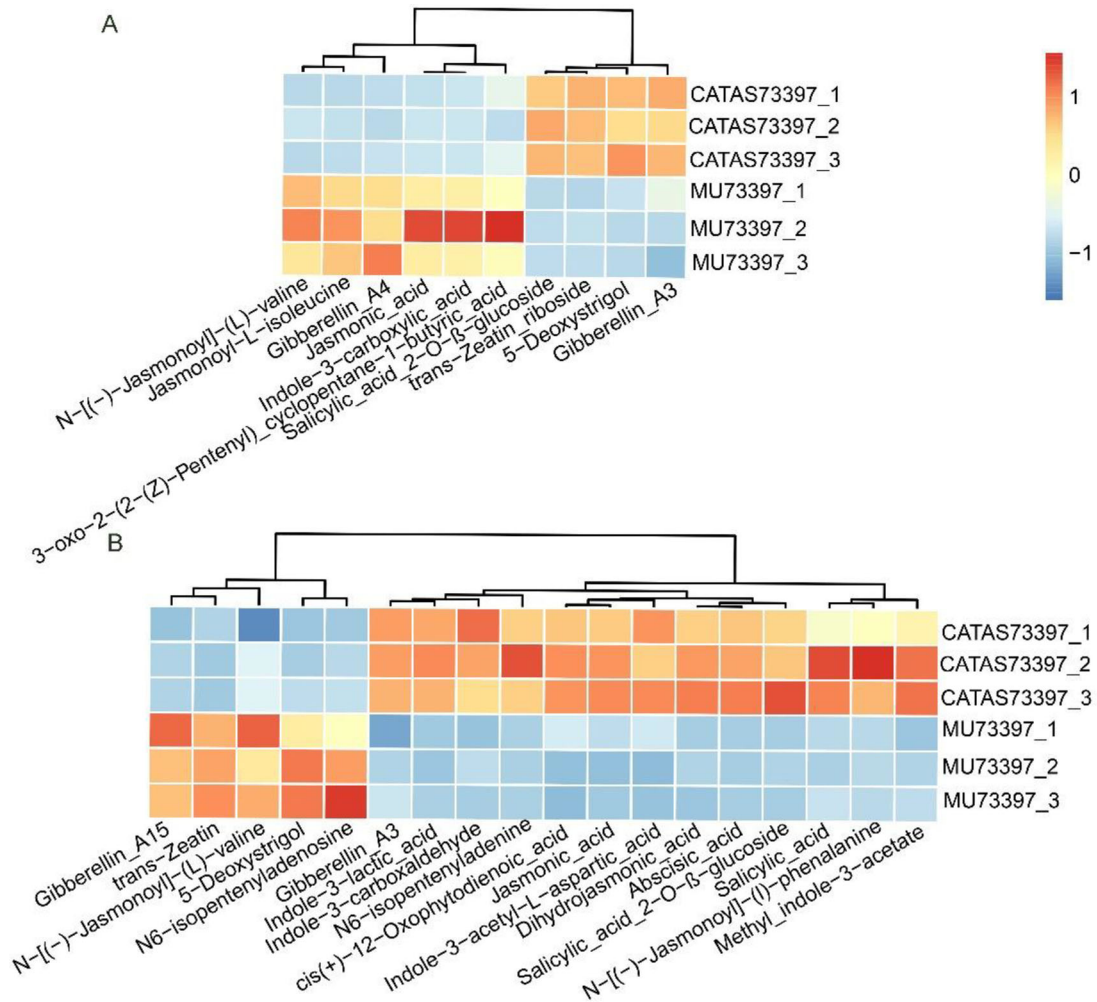


FIGURE 3 Differences in plant hormone content between MU73397 and CATAS73397. (A) Clustering heatmap of plant hormone content in the apices of MU73397 and CATAS73397. (B) Clustering heatmap of plant hormone content in the stems of MU73397 and CATAS73397.

clean reads was 40,998,669, yielding a total of 73.79 Gb of clean bases. The average Q20 value was 99.93%, the Q30 value was 96.52%, and the GC content was 43.29% (Table S2). These results demonstrate that the quality of the transcriptome sequencing data are high and suitable for subsequent analysis.

DEGs analysis revealed that there are 5313 DEGs between the xylem of MU73397 and CATAS73397, including 2488 upregulated DEGs and 2825 downregulated DEGs (Figure 4A,B). Between the phloem of MU73397 and CATAS73397, there are 16877 DEGs, including 965 upregulated DEGs and 722 downregulated DEGs (Figure 4A,C). Most of the DEGs are distributed in the xylem. To validate the reliability of the transcriptome data, six differentially expressed genes were randomly selected for qRT-PCR analysis (Figure 4D), including *HbFLA11*, which was later identified as a hub gene in subsequent analysis. The results showed that the gene expression patterns were consistent with the transcriptome data. This indicates that the transcriptome data are reliable and can be used for subsequent analysis.

To further explore the biological functions of the DEGs regulating the growth differences between MU73397 and CATAS73397, GO and KEGG enrichment analyses were performed. The GO analysis of the xylem DEGs revealed that two cell wall-related terms were significantly enriched in the top 20 GO terms, namely, “plant-type secondary cell wall biogenesis” and “plant-type cell wall” (Figure 5A). Additionally, the significantly enriched terms “beta-glucosidase activity,” “microtubule motor activity,” “microtubule,” and “integral component of plasma membrane” were all associated with cell wall formation. The GO analysis of the phloem DEGs showed that three cell wall-related terms were significantly enriched in the top 20 GO terms, including “plant-type secondary cell wall biogenesis,” “plant-type cell wall organization,” and “cell wall” (Figure 5B).

In the top 20 KEGG pathways significantly enriched in the DEGs of xylem, the most notable is the phenylpropanoid biosynthesis pathway, which is involved in lignin biosynthesis, making it a key pathway related to lignin (Figure 5C). In addition, two plant hormone-related

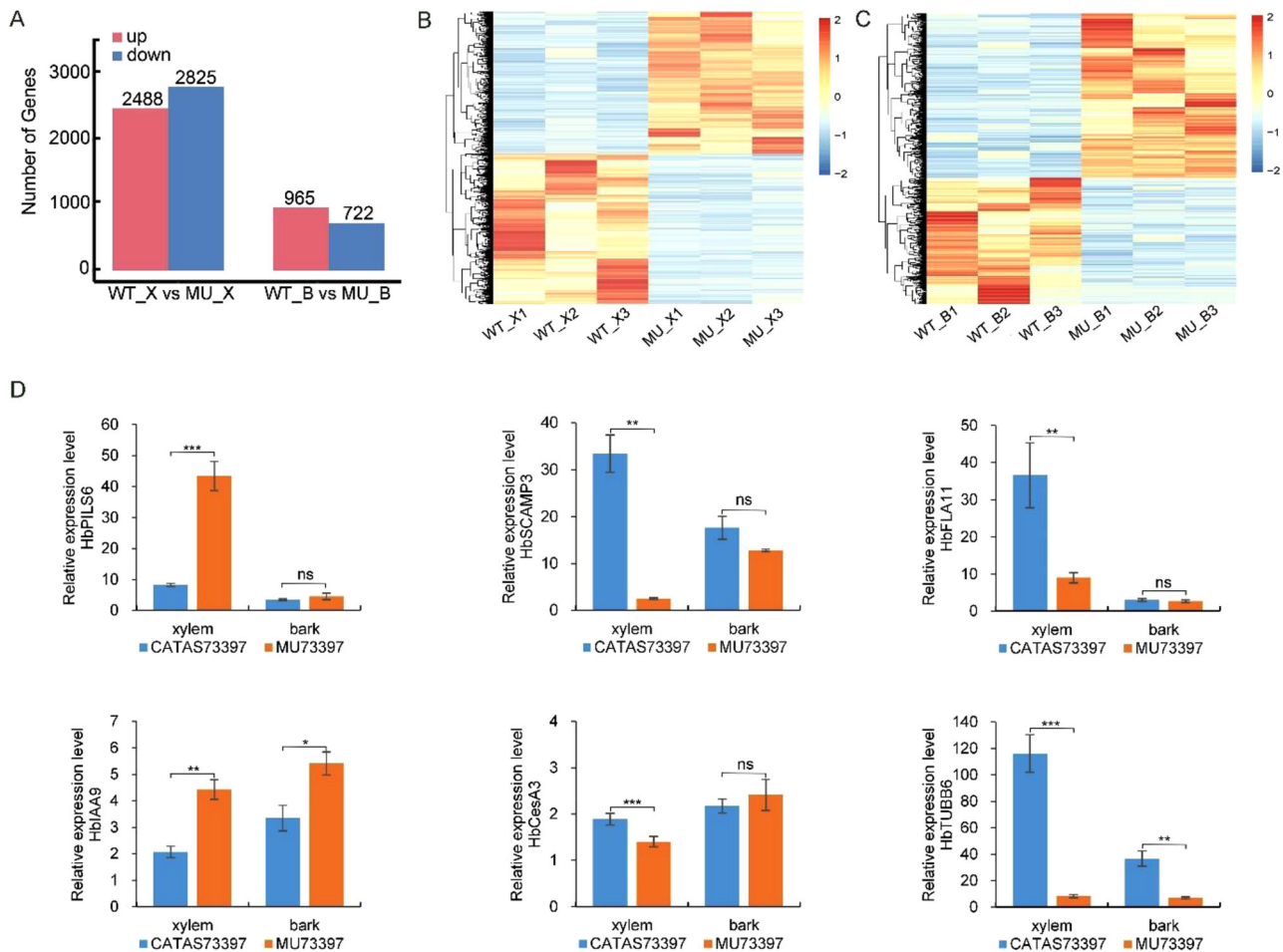


FIGURE 4 DEGs analysis and validation of transcriptome data. (A) Bar plot showing the number of upregulated and downregulated DEGs between the xylem of MU73397 and CATAS73397. (B) Cluster heatmap of DEGs between the xylem of MU73397 and CATAS73397. (C) Cluster heatmap of DEGs between the bark of MU73397 and CATAS73397. WT_X represent xylem of CATAS73397; WT_B represent bark of CATAS73397; MU_X represent xylem of MU73397; MU_B represent bark of MU73397. (D) qRT-PCR validation of six selected genes. * $p < 0.05$; ** $p < 0.01$; *** $p < 0.001$. ns, not significant.

pathways were significantly enriched, namely, plant hormone signal transduction and alpha-linolenic acid metabolism. Furthermore, four pathways related to carbohydrate synthesis and metabolism were enriched, including amino sugar and nucleotide sugar metabolism, starch and sucrose metabolism, interconversion of pentoses and glucuronic acid, and glycosaminoglycan degradation (Figure 5C). In the top 20 KEGG pathways significantly enriched in the DEGs of bark, the phenylpropanoid biosynthesis pathway, involved in lignin synthesis, was also enriched (Figure 5D). In addition, seven pathways related to plant hormone biosynthesis and signal transduction were significantly enriched, including plant hormone signal transduction, sesquiterpene and triterpene biosynthesis, brassinosteroid biosynthesis, indole alkaloid biosynthesis, tryptophan metabolism, diterpene biosynthesis, and cytokinin biosynthesis (Figure 5D). Moreover, pathways related to carbohydrate synthesis and metabolism, such as glycosaminoglycan degradation and sulfur-containing glucosinolates biosynthesis, were also significantly enriched (Figure 5D).

3.5 | Construction of a weighted gene co-expression network

WGCNA, or Weighted Gene Co-Expression Network Analysis, is an approach employed to clarify the patterns of correlation among genes throughout microarray samples (Langfelder & Horvath, 2008). In this study, transcriptome libraries of the apex and young stems of MU73397 and CATAS73397 were built, the phenotype data of plant height and girth were combined to explore the potential hub genes that regulated the trait of plant height in rubber tree, and all genes were divided into 39 modules through the WGCNA method (Figure 6A).

Through correlation analysis between these modules and plant height values, four main modules were screened out based on a significance criterion ($p < 0.05$). These modules were named turquoise ($r = -0.99$, $p = 0.0002$), blue ($r = 0.89$, $p = 0.02$), brown ($r = 0.88$, $p = 0.02$), and red ($r = 0.84$, $p = 0.04$) (Figure 6B). The findings from the phenotypic analyses indicated that the dwarf mutation observed in MU73397

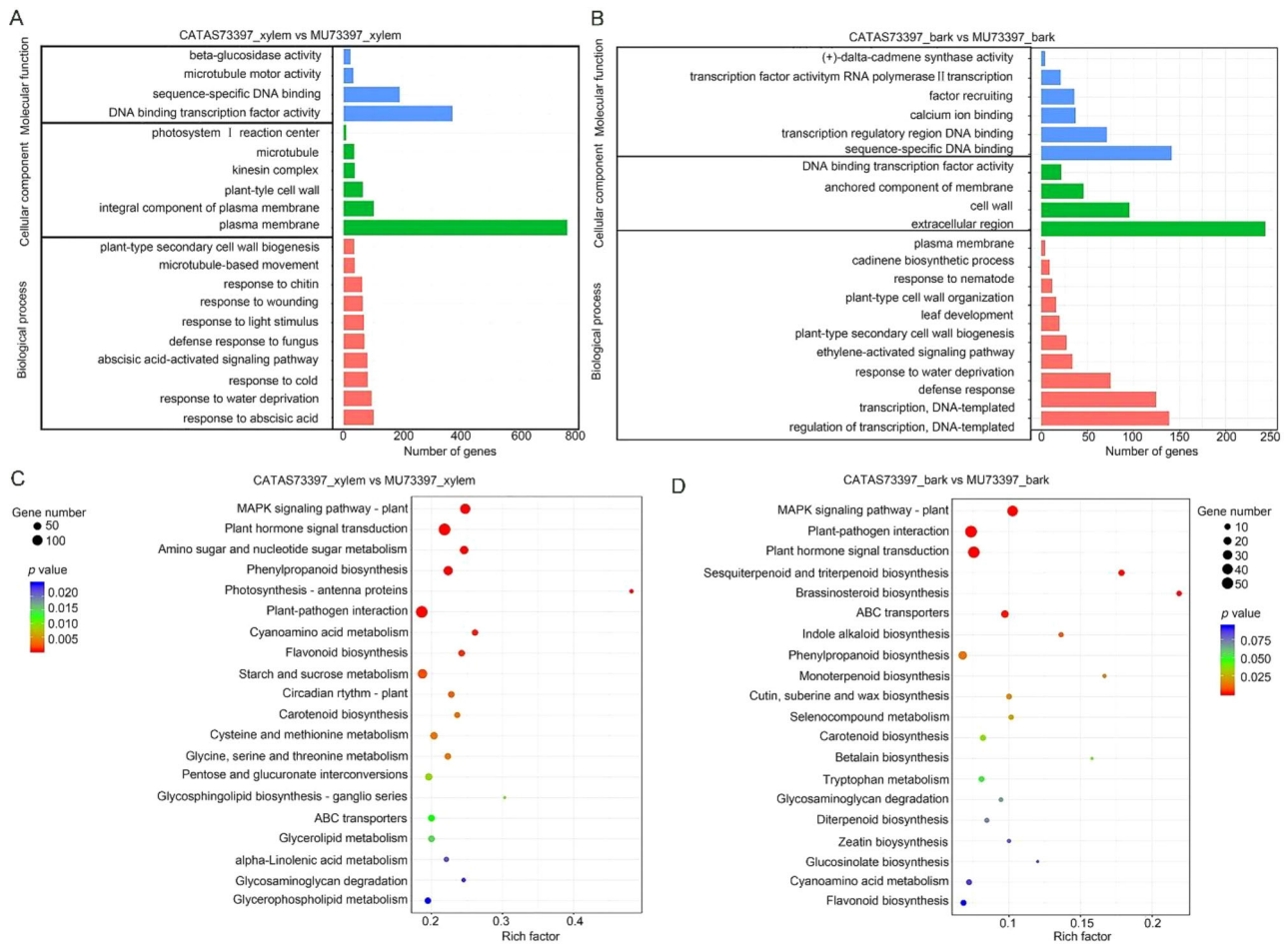


FIGURE 5 Top 20 GO and KEGG enrichment analysis of DEGs in the xylem and bark of MU73397 and CATAS73397. (A) Top 20 GO terms significantly enriched in the xylem. (B) Top 20 GO terms significantly enriched in the bark. (C) Top 20 KEGG pathways significantly enriched in the xylem. (D) Top 20 KEGG pathways significantly enriched in the bark.

could potentially be attributed to pathways associated with secondary cell wall formation and hormonal regulation. Of the four modules, the blue module distinguished itself by containing a significant proportion of DEGs associated with cell wall biosynthesis, cell proliferation, and hormone signaling. Therefore, it could be presumed that through further exploration and analyses of these DEGs, we might unveil potential hub genes responsible for regulating the plant height of rubber tree (Figure 6B).

3.6 | Identification of hub genes regulating plant height of rubber tree

To extract key genes from the blue module, we conducted the following analysis. First, we extracted the gene information of the top 500 nodes with the highest weight values in the blue module. These genes were analyzed using STRING, and a protein-protein interaction net-

work was constructed with Cytoscape. The importance of nodes and subnetworks was evaluated using the cytoHubba plugin, betweenness, degree, and maximal clique centrality algorithm, yielding nine candidate genes (Wan et al., 2024). These nine candidate genes are *FLA11* (scaffold2580_7757), *Tubulin Beta 1* (scaffold0563_496248), *TUBB6* (scaffold0056_919724), *CESA7* (cellulose synthase A 7; scaffold0470_894283), *Tubulin Alpha 4* (scaffold0054_1441312), *Laccase 7* (scaffold1051_280131), *Chitinase-like protein 2* (scaffold0624_169285), *Irregular xylem 9* (scaffold0029_724525), and *KOR* (korrigan; scaffold0346_48531) (Figure 7A).

Second, to confirm the reliability of these nine genes, we studied their expression in the rubber tree. The transcriptome analysis indicated that these nine genes were highly expressed in the xylem of CATAS73397 and down-regulated in the xylem of MU773397 (Figure 7B). This strongly suggests that these genes are involved in the regulation of tree height in rubber tree.

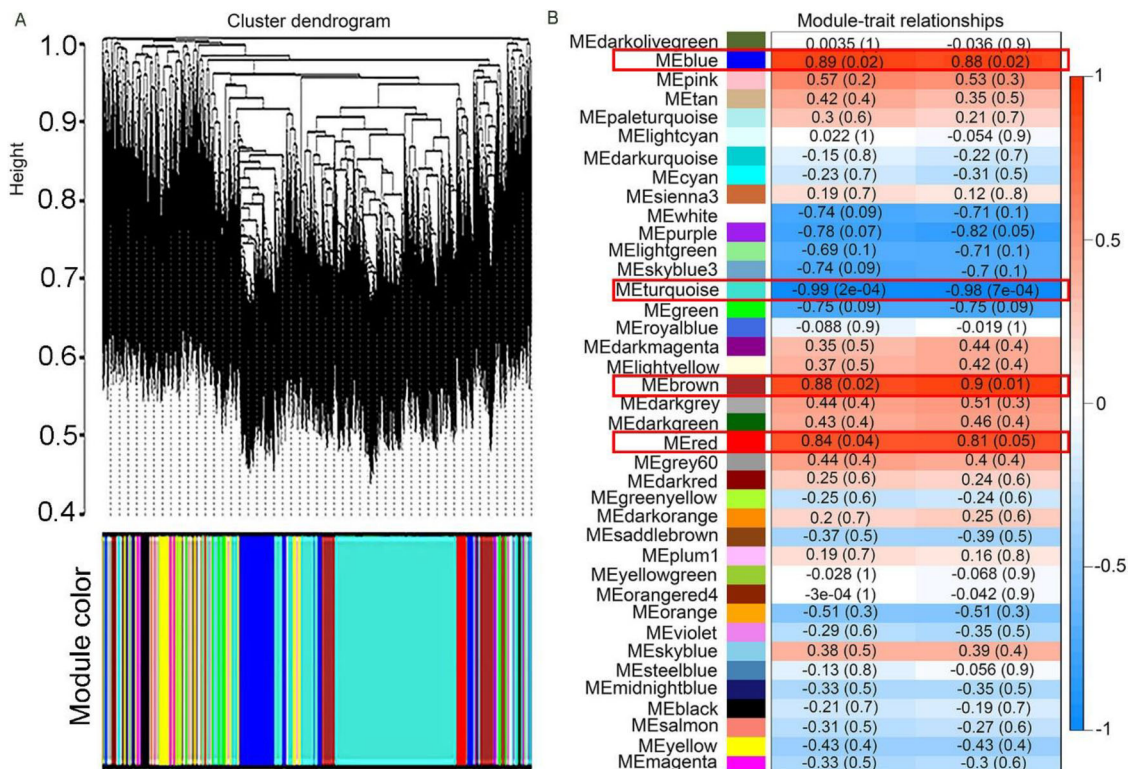


FIGURE 6 The dendrogram of network analysis showing modules identified by weighted gene co-expression network analysis (WGCNA). (A) Dendrogram plot with color annotation. (B) Module-traits weight correlations and corresponding *p*-values. The left panel shows the 39 modules. The color scale on the right shows module-traits correlation from -1 (blue) to 1 (red). The red frames indicate the four key modules.

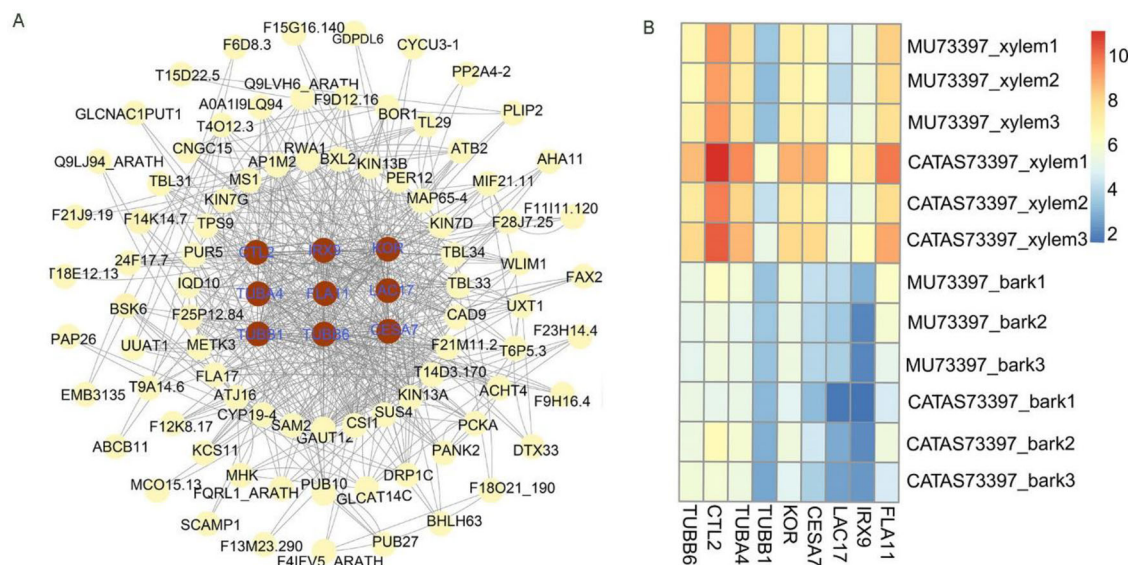


FIGURE 7 Identification of hub genes. (A) protein-protein interaction (PPI) network analysis. The top nine genes were identified using three algorithms—betweenness, degree, and maximal clique centrality (MCC)—provided by the Cytoscape plug-in. Represent the hub gene with a maroon shape. (B) Expression of the nine potential hub genes in the tissues of CATAS73397 and the dwarf mutant MU3397.

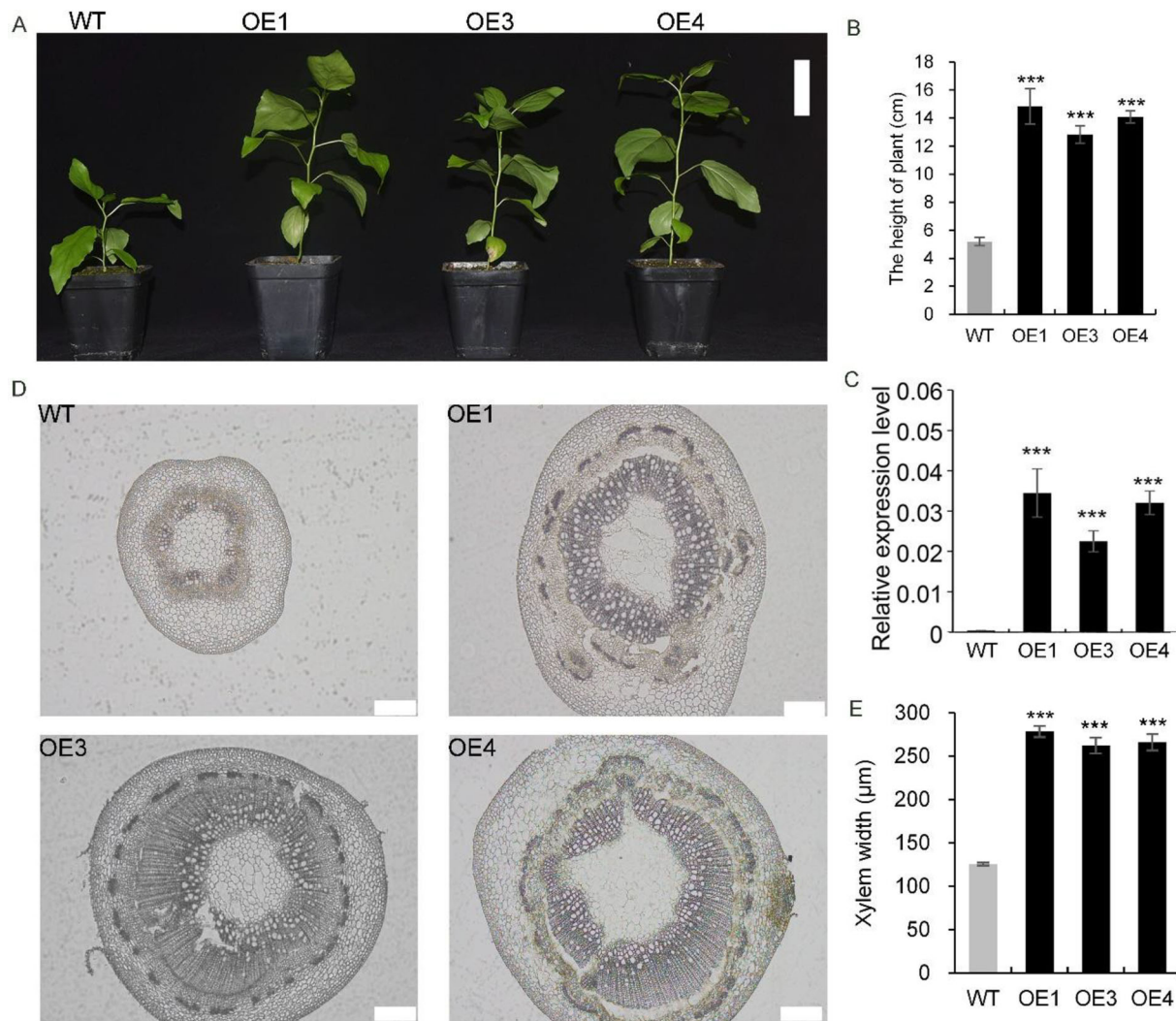


FIGURE 8 *HbFLA11* promotes plant height growth in poplar. (A) Images of *HbFLA11*-OE lines and wild-type poplar. Bar = 5 cm. (B) Plant height statistics of *HbFLA11*-OE lines and WT poplar. (C) Expression levels of *HbFLA11* in transgenic lines and WT poplar. (D) Microscopic observation of stems in *HbFLA11*-OE lines and WT poplar trees. Bar = 250 μm. (E) Statistical analysis of xylem width in stems of *HbFLA11*-OE lines and WT poplar trees. *** $p < 0.001$.

3.7 | Overexpression of *HbFLA11* improved plant height in transgenic poplar

We opted to conduct a functional validation of the *FLA11* gene, which encodes fasciclin-like arabinogalactan protein 11. To verify the function of *HbFLA11* in plant height, we overexpressed *HbFLA11* in transgenic poplar trees under the 35S promoter. We selected three independent *HbFLA11* overexpression lines (OE1, OE3, and OE4) for further analysis. Compared with WT) poplars, the *HbFLA11*-OE lines exhibited marked phenotypic differences, including a notable increase in plant height by approximately onefold (Figure 8A,B). qRT-PCR analysis confirmed a significant upregulation of *HbFLA11* expression in the transgenic lines (Figure 8C). These findings are consistent with the observed phenotypic changes and underscore the pivotal role of *HbFLA11* in regulating plant growth. To further investigate the effects of *HbFLA11* overexpression, paraffin sections

of stems 20 cm above the base were prepared from both *HbFLA11*-OE lines and WT poplars. Microscopic observations revealed that the stem diameter in *HbFLA11*-OE lines was significantly larger than that in WT poplars (Figure 8D). Statistical analysis demonstrated an approximate onefold increase in xylem width in *HbFLA11*-OE lines compared with WT poplars (Figure 8E). These results suggest that *HbFLA11* overexpression enhances cell wall development and promotes stem growth in poplars.

3.8 | *HbFLA11* affects GA biosynthesis and cell wall synthesis

To further elucidate the role of *HbFLA11* in regulating plant growth, we conducted qRT-PCR analysis to examine the expression profiles of genes associated with GA signaling and cell wall biosynthesis in *HbFLA11*-overexpressing

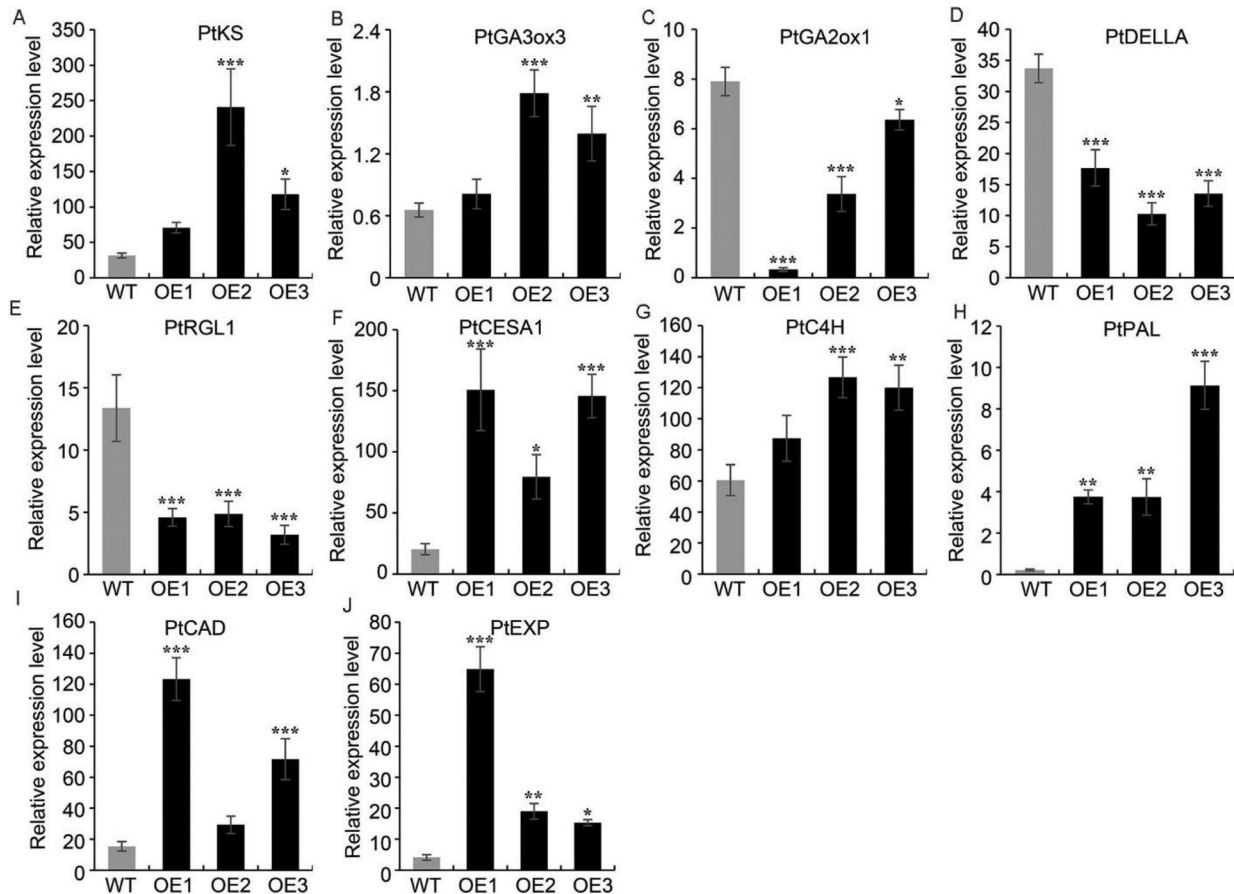


FIGURE 9 Expression of gibberellin-related and cell wall-related genes in transgenic poplars overexpressing *HbFLA11*. (A–E) Expression levels of gibberellin signaling-related genes. (F–J) Expression levels of cell wall biosynthesis-related genes. Error bars represent the standard deviations from three biological replicates. Asterisks denote the significance levels. * $p < 0.05$; ** $p < 0.01$; *** $p < 0.001$.

transgenic poplars. Most of these genes exhibited significant expression changes across three independent transgenic lines (Figure 9). Specifically, positive regulators of GA biosynthesis, such as *PtKS* and *PtGA3ox3*, were significantly upregulated in the transgenic plants, whereas negative regulators, including *PtGA2ox1*, *PtDELLA*, and *PtRGL1*, were markedly downregulated.

In addition, genes encoding key enzymes involved in cellulose and lignin biosynthesis, such as *PtCESA1*, *PtC4H*, *PtPAL*, and *PtCAD*, as well as *PtEXP*, which is crucial for cell expansion, also showed increased expression levels. These results suggest that *HbFLA11* overexpression enhances GA biosynthesis and signaling while simultaneously activating gene networks critical for cell wall thickening and structural integrity. Collectively, our findings indicate that *HbFLA11* positively regulates GA signaling pathways and cell wall biosynthesis, likely through direct or indirect mechanisms, thereby playing a pivotal role in modulating plant growth and development.

4 | DISCUSSION

Dwarf mutants of woody plants are rare and valuable germplasms that provide ideal material for exploring the molecular genetic mechanisms of tree growth. Elucidating the molecular mechanisms underlying dwarf mutations holds significant importance for breeding cultivars with desirable plant height traits (H. H. Huang et al., 2006). Chemical mutagenesis is one of the main ways to obtain dwarfing plant mutants (Kodym & Afza, 2003). The alkylating agent EMS is one of the chemical mutagens most commonly and widely used for random point mutations (Gillmor & Lukowitz, 2020). Moreover, EMS mutagenesis has broad potential in plant breeding (Kashif et al., 2023).

The mechanism of plant dwarfing is intricate and involves numerous genetic loci (Peng et al., 2023; Xu et al., 2023). Several dwarfing genes are closely related to plant hormone signaling pathways, such as GA, auxin, brassinolide, and other hormones (Depuydt & Hardtke, 2011). In the present study,

we obtained a dwarf mutant MU73397 by EMS mutation of the wild-type CATAS73397. The phenotypic identifications of MU73397 have revealed the differences in cell development, cell component content, and tissue hormone level between the mutant and its wild-type. Meanwhile, the subsequent comparative transcriptome study between MU73397 and CATAS73397 has provided molecular evidence for their phenotypic differences. The results also suggest that their height difference may be primarily caused by the differential expression of cell-wall-related genes regulated by GA, leading to differential deposition of xylem secondary wall components between MU73397 and CATAS73397. This study therefore aimed to enhance the understanding of the mechanisms governing the growth traits of rubber trees and provide candidate genes for the genetic improvement of rubber tree height.

4.1 | Reduced cell wall component accumulation contributes to dwarfism of MU73397

The xylem, as the primary structural component of the stem in woody plants, plays a crucial role in plant growth and is closely associated with plant height. In this study, SEM analysis revealed that the secondary xylem thickness in MU73397 was significantly lower than that in CATAS73397. In addition, the fiber cells in MU73397 were markedly smaller, and the cell wall thickness was reduced. The cellulose and lignin content in the stems of MU73397 was also significantly lower compared to CATAS73397. These findings suggest a potential link between xylem development and plant height in rubber trees. Therefore, the reduced accumulation of cell wall components may contribute to the dwarf phenotype of MU73397.

TUB, *CESA*, *FLA*, *LAC*, *CTL*, *IRX*, and *KOR* have been shown to regulate plant growth through their involvement in cell wall development. Tubulin (*TUB*) contributes to cell wall growth and plant development by participating in microtubule formation and cell wall deposition (Breviario et al., 2013; Swamy et al., 2015). The *CESA* genes are essential for cellulose biosynthesis, influencing cell wall structure and the plant's response to environmental stress (L. Huang et al., 2023; Nething et al., 2021). *FLA* proteins, particularly *FLA11*, regulate secondary cell wall development and respond to mechanical stimuli, modulating the synthesis of lignin and cellulose (Ma et al., 2022; H. Wang et al., 2015). Laccases (*LAC*) are involved in lignin polymerization, regulating lignin deposition in the cell wall (Hashemipetroudi et al., 2023; Hoffmann et al., 2020). The rice chitinase-like protein *BC15/OsCTL1* mediates cellulose biosynthesis and cell wall remodeling, contributing to plant growth and mechanical strength (B. Wu et al., 2012). *IRX* proteins are

responsible for xylan biosynthesis, significantly impacting cell wall structure and strength (Anders et al., 2023). Enzymes encoded by the *KOR* gene are crucial for cellulose synthesis and cell wall assembly (Maloney et al., 2012; Vain et al., 2014).

4.2 | Cell wall-related genes regulating plant height through hormonal signaling

This study found that the accumulation levels of various plant hormones in the stems and apices of MU73397 exhibited significant differences, especially the GA-related hormones (GA3 and GA4), which were significantly downregulated in both regions. The lack of GAs may be one of the key factors contributing to the dwarf phenotype of MU73397. In the process of cell wall development and plant growth, the downregulation of GA3 is closely associated with changes in the expression of multiple cell wall-related genes. Our results showed that GA3 content was significantly lower in the stems and apices of MU73397 compared to CATAS73397, and the expression levels of hub genes associated with the GA signaling pathway, such as *FLA*, *TUB*, *CESA*, and *CTL*, were also significantly reduced. Based on these findings, we hypothesize that these key cell wall-related genes may regulate plant height growth by participating in the GA signaling pathway.

The expression and activity of the *FLA*, *TUB*, *CESA*, and *CTL* genes are regulated by GA signaling. In poplar, the expression of *PtFLA* is negatively regulated by the GA signaling DELLA protein *PtRGA1* (Y. Zhang et al., 2023). Additionally, the *OsTUB4* gene in rice is influenced by GA3, with increased expression that contributes to regulating sheath growth (Yang et al., 2009). Under GA signaling, *CESA* genes promote cellulose synthesis by weakening the interaction between DELLA proteins and NAC transcription factors (Xiao et al., 2016). The expression and activity of *CTL* genes may also be regulated by GA levels, further affecting cell wall remodeling and plant mechanical strength (Wu & Bradford, 2003). These genes coordinate cell wall synthesis and reorganization in response to GA regulation, thereby promoting plant growth and development.

Furthermore, the differential accumulation of other hormones may further exacerbate the dwarf phenotype of MU73397. For instance, JA regulates plant stress responses and has a growth-inhibitory effect (Ghorbel et al., 2021; Janicka et al., 2023). In the apices of MU73397, JA-related hormones accumulate in high levels, which may inhibit plant growth and further aggravate the dwarf phenotype. Auxin plays a crucial role in promoting plant growth, particularly in cell elongation and division (Kubalová et al., 2024; Seo et al., 2021). However, in the stems of MU73397, auxin-related hormones are significantly downregulated, which may limit cell expansion and division, thus inhibiting nor-

mal plant growth and further contributing to the dwarf phenotype.

4.3 | Overexpression of *HbFLA11* increased lignification and plant height of poplar

This study, employing WGCNA and STRING analyses, identified nine potential key regulatory genes within the blue module of the rubber tree MU73397 that influence plant height growth. The *HbFLA11* gene was selected for functional validation. Overexpression of *HbFLA11* led to a more than onefold increase in the height of transgenic poplar trees. The *FLA* family has been identified and studied in various plants, including tomato (Yao et al., 2023), willow (Y. Zhang et al., 2023), *Arabidopsis* (Ma et al., 2023), and rice (Zhou et al., 2022). While evidence suggests that the *FLA* family is involved in secondary wall formation (Liu et al., 2020), its role in regulating plant height growth remains unclear.

Microscopic analysis revealed that overexpression of *HbFLA11* leads to increased stem girth and enhanced development of the xylem in poplars, indicating its positive role in promoting cell growth. At the molecular level, these morphological changes are associated with significant alterations in the expression of genes involved in GA signaling and cell wall biosynthesis, further elucidating role of *HbFLA11* in fine-tuning plant growth through modulation of these pathways. Consistent with previous observations, the dwarf phenotype of MU73397 is linked to reduced GA content, decreased cellulose and lignin levels, and a marked downregulation of the *HbFLA11* gene. Overall, our data suggest that *HbFLA11* may be involved in the synthesis and signaling of GAs, promoting cell proliferation, accelerating cell wall maturation, and influencing hormone balance, highlighting its multifaceted role in regulating the growth and development of poplar.

The nine candidate genes, including *HbFLA11*, are involved in regulating plant height growth. In future rubber tree breeding programs, modulating these genes could help control tree height and enhance growth stability, thereby improving wind resistance to mitigate the impact of natural disasters (e.g., typhoons) on rubber tree growth.

5 | CONCLUSIONS

In this study, the dwarf phenotype of the MU73397 rubber tree mutant is primarily caused by delayed xylem development, reduced levels of cell wall components (cellulose and lignin), and alterations in the cell wall structure. These factors collectively contribute to the significant reduction in plant height and stem diameter. The changes in phenotype are closely associated with differences in plant hormone levels, particularly the downregulation of GAs (GA3 and GA4) in the

apex and stems of MU73397, which may inhibit cell expansion and division. Transcriptome analysis further revealed the involvement of several key biological pathways in the formation of the dwarf phenotype in MU73397, including phenylpropanoid biosynthesis and plant hormone signal transduction. WGCNA analysis identified nine hub genes that may play an important role in regulating plant height. Functional validation experiments demonstrated that overexpression of *HbFLA11* promotes growth in poplar, increases plant height, and enhances cell wall development by regulating GA signaling and cell wall biosynthesis genes. Overall, these findings provide important insights into the genetic mechanisms and hormonal regulation of the rubber tree dwarf phenotype and offer potential strategies for improving growth traits in rubber tree.

AUTHOR CONTRIBUTIONS

Baoyi Yang: Conceptualization; formal analysis; investigation; validation; writing—original draft; writing—review and editing. **Yuanyuan Zhang:** Conceptualization; data curation; formal analysis; investigation; writing—review and editing. **Weiguo Li:** Conceptualization; data curation; formal analysis; investigation; writing—review and editing. **Xiao Huang:** Conceptualization; data curation; formal analysis; investigation; writing—review and editing. **Xinsheng Gao:** Conceptualization; data curation; formal analysis; investigation; writing—review and editing. **Juncang Qi:** Data curation; methodology; project administration; supervision; writing—review and editing. **Xiangjun Wang:** Formal analysis; funding acquisition; visualization; writing—review and editing.

ACKNOWLEDGMENTS

This research was funded by the Central Public-Interest Scientific Institution Basal Research Fund (No. 1630032022007), Special Fund for Hainan Excellent Team ‘Rubber Genetics and Breeding’ (No. 20210203), and National Key R & D Program of China (No. 2019YFD1000500).

CONFLICT OF INTEREST STATEMENT

The authors declare no conflicts of interest.

DATA AVAILABILITY STATEMENT

The datasets generated and/or analyzed during the course of this study are accessible in the NCBI database under the accession number PRJNA1112341. Original contributions of this study, beyond the datasets, are included within the article and its Supplementary material. For any further inquiries or requests, please direct them to the corresponding author.

ORCID

Juncang Qi  <https://orcid.org/0000-0002-2773-5416>

Xiangjun Wang  <https://orcid.org/0009-0007-4929-1557>

REFERENCES

- Anders, N., Wilson, L. F. L., Sorieul, M., Nikolovski, N., & Dupree, P. (2023). β -1,4-Xylan backbone synthesis in higher plants: How complex can it be? *Frontiers in Plant Science*, *13*, 1076298. <https://doi.org/10.3389/fpls.2022.1076298>
- Balai, H. K., Sahu, A., & Bairwa, K. C. (2023). Sources of output growth and variability of natural rubber in India. *Asian Journal of Agricultural Extension, Economics & Sociology*, *41*(6), 147–152. <https://doi.org/10.9734/ajaees/2023/v41i61932>
- Breviario, D., Gianì, S., & Morello, L. (2013). Multiple tubulins: Evolutionary aspects and biological implications. *The Plant Journal*, *75*(2), 202–218. <https://doi.org/10.1111/tpj.12243>
- Chen, Z. X., Zhao, J. W., Zhai, Q. L., & Li, W. G. (2012). Mutation method for rubber secondary embryo induced by EMS. *Chinese Journal of Tropical Agriculture*, *32*, 32–35. (In Chinese).
- Cheng, H., Song, X., Hu, Y., Wu, T., Yang, Q., An, Z., Feng, S., Deng, Z., Wu, W., Zeng, X., Tu, M., Wang, X., & Huang, H. (2023). Chromosome-level wild *Hevea brasiliensis* genome provides new tools for genomic-assisted breeding and valuable loci to elevate rubber yield. *Plant Biotechnology Journal*, *21*(5), 1058–1072. <https://doi.org/10.1111/pbi.14018>
- Conson, A. R. O., Taniguti, C. H., Amadeu, R. R., Andreotti, I. A. A., & de Souza, L. M. (2018). High-resolution genetic map and QTL analysis of growth-related traits of *Hevea brasiliensis* cultivated under suboptimal temperature and humidity conditions. *Frontiers in Plant Science*, *9*, 1255. <https://doi.org/10.3389/fpls.2018.01255>
- Depuydt, S., & Hardtke, C. S. (2011). Hormone signalling crosstalk in plant growth regulation. *Current Biology*, *21*, R365–R373. <https://doi.org/10.1016/j.cub.2011.03.013>
- Francisco, F. R., Aono, A. H., da Silva, C. C., Gonçalves, P. S., Scaloppi Junior, E. J., Le Guen, V., Fritsche-Neto, R., Souza, L. M., & Souza, de, A. P. (2021). Unravelling rubber tree growth by integrating GWAS and biological network-based approaches. *Frontiers in Plant Science*, *12*, 768589. <https://doi.org/10.3389/fpls.2021.768589>
- GB/T 2677.10-95. (1995). *Fibrous raw material-Determination of holocellulose*. National Standard of the People's Republic of China. (In Chinese).
- GB/T 2677.1-93. (1993). *Fibrous raw material of sampling for analysis*. National Standard of the People's Republic of China. (In Chinese).
- GB/T 2677.6-94. (1994). *Fibrous raw material-Determination of solvent extractives*. National Standard of the People's Republic of China. (In Chinese).
- GB/T 2677.8-94. (1994). *Fibrous raw material-Determination of acid-insoluble lignin*. National Standard of the People's Republic of China. (In Chinese).
- Ghorbel, M., Brini, F., Sharma, A., & Landi, M. (2021). Role of jasmonic acid in plants: The molecular point of view. *Plant Cell Reports*, *40*(8), 1471–1494. <https://doi.org/10.1007/s00299-021-02687-4>
- Gillmor, C. S., & Lukowitz, W. (2020). EMS mutagenesis of Arabidopsis seeds. In M. Bayer (Ed.), *Methods in Molecular Biology*, *2122*, 15–23. https://doi.org/10.1007/978-1-0716-0342-0_2
- Hashemipetroudi, S. H., Arab, M., Heidari, P., & Kuhlmann, M. (2023). Genome-wide analysis of the laccase (LAC) gene family in *Aeluropus littoralis*: A focus on identification, evolution and expression patterns in response to abiotic stresses and ABA treatment. *Frontiers in Plant Science*, *14*, 1112354. <https://doi.org/10.3389/fpls.2023.1112354>
- Hoffmann, N., Benske, A., Betz, H., Schuetz, M., & Samuels, A. L. (2020). Laccases and peroxidases co-localize in lignified secondary cell walls throughout stem development. *Plant Physiology*, *184*(2), 806–822. <https://doi.org/10.1104/pp.20.00473>
- Hua, Y., Huang, T. D., & Huang, H. (2010). Micropropagation of self-rooting juvenile clones by secondary somatic embryogenesis in *Hevea brasiliensis*. *Plant Breeding*, *129*(2), 202–207. <https://doi.org/10.1111/j.1439-0523.2009.01663.x>
- Huang, H. H., Tong, Z. K., Zhu, Y. Q., Gao, Y. H., Xu, C. S., & He, F. J. (2006). Proteome study of dwarf mutant in *Cunninghamia lanceolata* by 2D-DIGE. *Journal of Zhejiang A&F University*, *23*, 265–269. (In Chinese).
- Huang, L., Zhang, W., Li, X., Staiger, C. J., & Zhang, C. (2023). Point mutations in the catalytic domain disrupt cellulose synthase (CESA6) vesicle trafficking and protein dynamics. *Plant Cell*, *35*(7), 2654–2677. <https://doi.org/10.1093/plcell/koad110>
- Janicka, M., Reda, M., Mroczko, E., Wdowikowska, A., & Kabała, K. (2023). Jasmonic acid effect on *Cucumis sativus* L. growth is related to inhibition of plasma membrane proton pump and the uptake and assimilation of nitrates. *Cells*, *12*(18), 2263. <https://doi.org/10.3390/cells12182263>
- Kashif, S. Z., Aslam, M., Ahmed, Z., Saleem, F., Alghabari, F., Alsamadany, H., Alzahrani, H. A. S., & Awan, F. S. (2023). Development and genomic characterization of EMS induced mutant population of *Zea mays* L. *Plant Genetic Resources*, *20*(3), 188–193. <https://doi.org/10.1017/s1479262123000023>
- Kodym, A., & Afza, R. (2003). Physical and chemical mutagenesis. *Methods in Molecular Biology*, *236*, 189–204. <https://doi.org/10.1385/1-59259-413-1:189>
- Kubalová, M., Müller, K., Dobrev, P. I., Rizza, A., Jones, A. M., & Fendrych, M. (2024). Auxin co-receptor IAA17/AXR3 controls cell elongation in *Arabidopsis thaliana* root solely by modulation of nuclear auxin pathway. *New Phytologist*, *241*(6), 2448–2463. <https://doi.org/10.1111/nph.19557>
- Langfelder, P., & Horvath, S. (2008). WGCNA: An R package for weighted correlation network analysis. *BMC Bioinformatics*, *9*, 559. <https://doi.org/10.1186/1471-2105-9-559>
- Lau, N. S., Makita, Y., Kawashima, M., Taylor, T. D., Kondo, S., Othman, A. S., Shu-Chien, A. C., & Matsui, M. (2016). The rubber tree genome shows expansion of gene family associated with rubber biosynthesis. *Scientific Reports*, *6*, 28594. <https://doi.org/10.1038/srep28594>
- Li, Z. F., Guo, Y., Ou, L., Hong, H., Wang, J., Liu, Z. X., Guo, B., Zhang, L., & Qiu, L. (2018). Identification of the dwarf gene GmDW1 in soybean (*Glycine max* L.) by combining mapping-by-sequencing and linkage analysis. *Theoretical and Applied Genetics*, *131*(5), 1001–1016. <https://doi.org/10.1007/s00122-017-3044-8>
- Liu, E., MacMillan, C. P., Shafee, T., Ma, Y., Ratcliffe, J., van de Meene, A., Bacic, A., Humphries, J., & Johnson, K. L. (2020). Fasciclin-like arabinogalactan-protein 16 (FLA16) is required for stem development in *Arabidopsis*. *Frontiers in Plant Science*, *11*, 615392. <https://doi.org/10.3389/fpls.2020.615392>
- Ma, Y., MacMillan, C. P., de Vries, L., Mansfield, S. D., Hao, P., Ratcliffe, J., Bacic, A., & Johnson, K. L. (2022). FLA11 and FLA12 glycoproteins fine-tune stem secondary wall properties in response to mechanical stresses. *New Phytologist*, *233*(4), 1750–1767. <https://doi.org/10.1111/nph.17898>
- Ma, Y., Shafee, T., Mudiyanse, A. M., Ratcliffe, J., MacMillan, C. P., Mansfield, S. D., Bacic, A., & Johnson, K. L. (2023). Distinct functions of FASCILIN-LIKE ARABINO GALACTAN PROTEINS

- relate to domain structure. *Plant Physiology*, 192(1), 119–132. <https://doi.org/10.1093/plphys/kiad097>
- Maloney, V. J., Samuels, A. L., & Mansfield, S. D. (2012). The endo-1, 4- β -glucanase Korrigan exhibits functional conservation between gymnosperms and angiosperms and is required for proper cell wall formation in gymnosperms. *New Phytologist*, 193(4), 1076–1087. <https://doi.org/10.1111/j.1469-8137.2011.03998.x>
- Mortazavi, A., Williams, B. A., McCue, K., Schaeffer, L., & Wold, B. (2008). Mapping and quantifying mammalian transcriptomes by RNA-Seq. *Nature Methods*, 5(7), 621–628. <https://doi.org/10.1038/nmeth.1226>
- Nething, D. B., Sukul, A., Mishler-Elmore, J. W., & Held, M. A. (2021). Posttranscriptional regulation of cellulose synthase genes by small RNAs derived from cellulose synthase antisense transcripts. *Plant Direct*, 5(9), e347. <https://doi.org/10.1002/pld3.347>
- Peng, S., Liu, Y., Xu, Y., Zhao, J., Gao, P., Liu, Q., Yan, S., Xiao, Y., Zuo, S. M., & Kang, H. (2023). Genome-wide association study identifies a plant-height—Associated gene *OsPG3* in a population of commercial rice varieties. *International Journal of Molecular Sciences*, 24(14), 11454. <https://doi.org/10.3390/ijms241411454>
- Pootakham, W., Sonthirod, C., Naktang, C., Ruang-Areerate, P., Yoocha, T., Sangsrakru, D., Theerawattanasuk, K., Rattanawong, R., Lekawipat, N., & Tangphatsornruang, S. (2017). De novo hybrid assembly of the rubber tree genome reveals evidence of paleotetraploidy in *Hevea* species. *Scientific Reports*, 7, 41457. <https://doi.org/10.1038/srep41457>
- Priyadarshan, P. M. (2022). Molecular markers to devise predictive models for juvenile selection in *Hevea* rubber. *Plant Breeding*, 141(2), 159–183. <https://doi.org/10.1111/pbr.13001>
- Rahman, A. Y. A., Usharraj, A. O., Misra, B. B., Thottathil, G. P., Jayasekaran, K., Feng, Y., Hou, S., Ong, S. Y., Ng, F. L., Lee, L. S., Tan, H. S., Sakaff, M. K. L. M., Teh, B. S., Khoo, B. F., Badai, S. S., Aziz, N. A., Yuryev, A., Knudsen, B., Dionne-Laporte, A., ... Alam, M. (2013). Draft genome sequence of the rubber tree *Hevea brasiliensis*. *BMC Genomics*, 14, Article 75. <https://doi.org/10.1186/1471-2164-14-75>
- Rosa, J. R. B. F., Mantello, C. C., Garcia, D., De Souza, L. M., Da Silva, C. C., Gazaffi, R., Da Silva, C. C., Toledo-Silva, G., Cubry, P., Garcia, A. A. F., De Souza, A. P., & Le Guen, V. (2018). QTL detection for growth and latex production in a full-sib rubber tree population cultivated under suboptimal climate conditions. *BMC Plant Biology*, 18(1), Article 223. <https://doi.org/10.1186/s12870-018-1450-y>
- Seo, D. H., Jeong, H., Choi, Y. D., & Jang, G. (2021). Auxin controls the division of root endodermal cells. *New Phytologist*, 187(3), 1577–1586. <https://doi.org/10.1093/plphys/kiab341>
- Swamy, P. S., Hu, H., Pattathil, S., Maloney, V. J., Xiao, H., Xue, L. J., Chung, J. D., Johnson, V. E., Zhu, Y., Peter, G. F., Hahn, M. G., Mansfield, S. D., Harding, S. A., & Tsai, C. J. (2015). Tubulin perturbation leads to unexpected cell wall modifications and affects stomatal behaviour in *Populus*. *Journal of Experimental Botany*, 66(20), 6507–18. <https://doi.org/10.1093/jxb/erv383>
- Tang, C., Yang, M., Fang, Y., Luo, Y., Gao, S., Xiao, X., An, Z., Zhou, B., Zhang, B., Tan, X., Yeang, H. Y., Qin, Y., Yang, J., Lin, Q., Mei, H., Montoro, P., Long, X., Qi, J., Hua, Y., ... Huang, H. (2016). The rubber tree genome reveals new insights into rubber production and species adaptation. *Nature Plants*, 2, Article 16073. <https://doi.org/10.1038/nplants.2016.73>
- Taylor-Teeples, M., Lin, L., de Lucas, M., Turco, G., Toal, T. W., Gaudinier, A., Young, N. F., Trabucco, G. M., Veling, M. T., Lamothe, R., Handakumbura, P. P., Xiong, G., Wang, C., Corwin, J., Tsoukalas, A., Zhang, L., Ware, D., Pauly, M., Kliebenstein, D. J., ... Brady, S. M. (2015). An *Arabidopsis* gene regulatory network for secondary cell wall synthesis. *Nature*, 517(7536), 571–575. <https://doi.org/10.1038/nature14099>
- Tian, Z., Zhang, Y., Zhu, L., Jiang, B., Wang, H., Gao, R., Friml, J., & Xiao, G. (2022). Strigolactones act downstream of gibberellins to regulate fiber cell elongation and cell wall thickness in cotton (*Gossypium hirsutum*). *Plant Cell*, 34(12), 4816–4839. <https://doi.org/10.1093/plcell/koac270>
- Vain, T., Crowell, E. F., Timpano, H., Biot, E., Desprez, T., Mansoori, N., Trindade, L. M., Pagant, S., Robert, S., Höfte, H., Gonneau, M., & Vernhettes, S. (2014). The cellulase KORRIGAN is part of the cellulose synthase complex. *Plant Physiology*, 165(4), 1521–1532. <https://doi.org/10.1104/pp.114.241216>
- Wan, Y., Wang, Y., Xu, S., Du, H., & Liu, Z. (2024). Identification of the role of pyroptosis-related genes in chronic rhinosinusitis based on WGCNA. *Heliyon*, 10, e22944. <https://doi.org/10.1016/j.heliyon.2023.e22944>
- Wang, G. L., Que, F., Xu, Z. S., Wang, F., & Xiong, A. S. (2017). Exogenous gibberellin enhances secondary xylem development and lignification in carrot taproot. *Protoplasma*, 254(2), 839–848. <https://doi.org/10.1007/s00709-016-0995-6>
- Wang, H., Jiang, C., Wang, C., Yang, Y., Yang, L., Gao, X., & Zhang, H. (2015). Antisense expression of the fasciclin-like arabinogalactan protein *FLA6* gene in *Populus* inhibits expression of its homologous genes and alters stem biomechanics and cell wall composition in transgenic trees. *Journal of Experimental Botany*, 66(5), 1291–302. <https://doi.org/10.1093/jxb/eru479>
- Wang, H., Jin, Y., Wang, C., Li, B., Jiang, C., Sun, Z., Zhang, Z., Kong, F., & Zhang, H. (2017). Fasciclin-like arabinogalactan proteins, PtFLAs, play important roles in GA-mediated tension wood formation in *Populus*. *Scientific Reports*, 7(1), 6182. <https://doi.org/10.1038/s41598-017-06473-9>
- Wang, X. J., Zeng, X. Z., Wang, Y. J., Huang, X., Zhang, Y. Y., & Li, W. G. (2018). Wood ultrastructure observation of rubber tree (*Hevea brasiliensis* Muell. Arg.) young stem. *Bulletin of Botanical Research*, 38, 876–885. <https://doi.org/10.7525/j.issn.1673-5102.2018.06.011>
- Wu, B., Zhang, B., Dai, Y., Zhang, L., Shang-Guan, K., Peng, Y., Zhou, Y., & Zhu, Z. (2012). Brittle culm15 encodes a membrane-associated chitinase-like protein required for cellulose biosynthesis in rice. *Plant Physiology*, 159(4), 1440–52. <https://doi.org/10.1104/pp.112.195529>
- Wu, C. T., & Bradford, K. J. (2003). Class I chitinase and β -1, 3-glucanase are differentially regulated by wounding, methyl jasmonate, ethylene, and gibberellin in tomato seeds and leaves. *Plant Physiology*, 133(1), 263–273. <https://doi.org/10.1104/pp.103.024687>
- Wu, W., Zhang, X., Deng, Z., An, Z., Huang, H., Li, W., & Cheng, H. (2022). Ultrahigh-density genetic map construction and identification of quantitative trait loci for growth in rubber tree (*Hevea brasiliensis*). *Industrial Crops and Products*, 178, 114560. <https://doi.org/10.1016/j.indcrop.2022.114560>
- Xiao, G. H., Wang, K., Huang, G., & Zhu, Y. X. (2016). Genome-scale analysis of the cotton KCS gene family revealed a binary mode of action for gibberellin A regulated fiber growth. *Journal of Integrative Plant Biology*, 58(6), 577–89. <https://doi.org/10.1111/jipb.12429>
- Xie, X., Zhang, Y., Xu, L., Xiong, H., Xie, Y., Zhao, L., Gu, J., Li, H., Zhang, J., Ding, Y., Zhao, S., Guo, H., & Liu, L. (2024). Mapping of dwarfing gene and identification of mutant allele on plant height in

- wheat. *Molecular Breeding*, 44, Article 79. <https://doi.org/10.1007/s11032-024-01515-3>
- Xu, D., Jia, C., Lyu, X., Yang, T., Qin, H., Wang, Y., Hao, Q., Liu, W., Dai, X., Zeng, J., Zhang, H., Xia, X., He, Z., Cao, S., & Ma, W. (2023). In silico curation of QTL-rich clusters and candidate gene identification for plant height of bread wheat. *The Crop Journal*, 11(5), 1480–1490. <https://doi.org/10.1016/j.cj.2023.05.007>
- Yang, G., Jan, A., & Komatsu, S. (2009). Characterization of β -tubulin 4 regulated by gibberellins in rice leaf sheath. *Biologia Plantarum*, 53, 422–428. <https://doi.org/10.1007/s10535-009-0081-4>
- Yao, K., Yao, Y., Ding, Z., Pan, X., Zheng, Y., Huang, Y., Zhang, Z., Li, A., Wang, C., Li, C., & Liao, W. (2023). Characterization of the *FLA* gene family in tomato (*Solanum lycopersicum* L.) and the expression analysis of *SIFLAs* in response to hormone and abiotic stresses. *International Journal of Molecular Sciences*, 24(22), 16063. <https://doi.org/10.3390/ijms242216063>
- Zhang, D., Xu, Z., Cao, S., Chen, K., Li, S., Liu, X., Gao, C., Zhang, B., & Zhou, Y. (2018). An uncanonical CCCH-tandem zinc-finger protein represses secondary wall synthesis and controls mechanical strength in rice. *Molecular Plant*, 11(1), 63–174. <https://doi.org/10.1016/j.molp.2017.11.004>
- Zhang, Y., Zhou, F., Wang, H., Chen, Y., Yin, T., & Wu, H. (2023). Genome-wide comparative analysis of the fasciclin-like arabinogalactan proteins (FLAs) in Salicacea and identification of secondary tissue development-related genes. *International Journal of Molecular Sciences*, 24(2), 1481. <https://doi.org/10.3390/ijms24021481>
- Zhou, D., Zou, T., Zhang, K., Xiong, P., Zhou, F., Chen, H., Li, G., Zheng, K., Han, Y., Peng, K., Zhang, X., Yang, S., Deng, Q., Wang, S., Zhu, J., Liang, Y., Sun, C., Yu, X., Liu, H., ... Li, S. (2022). *s* encodes a fasciclin-like arabinogalactan protein required for male fertility in rice. *Journal of Integrative Plant Biology*, 64, 1430–1447. <https://doi.org/10.1111/jipb.13271>

SUPPORTING INFORMATION

Additional supporting information can be found online in the Supporting Information section at the end of this article.

How to cite this article: Yang, B., Zhang, Y., Li, W., Huang, X., Gao, X., Qi, J., & Wang, X. (2025). Phenotypic and transcriptomic analysis reveals key genes associated with plant height in rubber tree and functional characterization of the candidate gene *HbFLA11*. *The Plant Genome*, 18, e70048. <https://doi.org/10.1002/tpg2.70048>